Biophysical Chemistry 205 (2015) 9–15

Contents lists available at ScienceDirect

Biophysical Chemistry

journal homepage: http://www.elsevier.com/locate/biophyschem

Effects of guanine bases at the central loop on stabilization of the quadruplex DNAs and their interactions with *Meso*-tetrakis(*N*-methylpyridium-4-yl)porphyrin

Sun Hee Jeon [a], Jihye Moon [a], Myung Won Lee [a,b], Seog K. Kim [a,*]

[a] Department of Chemistry, Yeungnam University, 214 Dae-dong, Gyeongsan City, Gyeong-buk, 712-749, Republic of Korea
[b] Department of Chemistry, Pukyoung National University, Pusan, 608-737, Republic of Korea

HIGHLIGHTS

- Thermal stability of a quadruplex, 5′ $G_2T_2G_2TXTG_2T_2G_2$ (X = A, I or G), was investigated.
- Thermal stability is lowest when X = A.
- Central G or I base can form hydrogen bond with G bases in upper G-quartet.
- Replacement of G base did not affect the spectral properties of TMPyP.

GRAPHICAL ABSTRACT

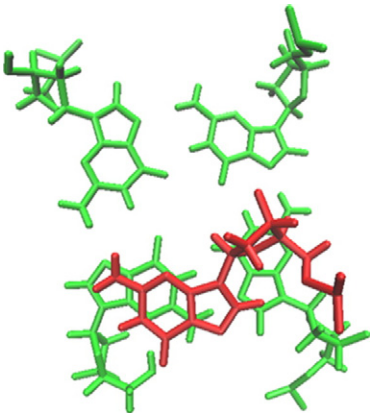

ARTICLE INFO

Article history:
Received 1 April 2015
Received in revised form 28 May 2015
Accepted 29 May 2015
Available online 3 June 2015

Keywords:
DNA
Quadruplex
Circular dichroism
Porphyrin
Theoretical calculation

ABSTRACT

The thermal stability of the G-quadruplex formed from the thrombin-binding aptamer, 5′$G_2T_2G_2TGTG_2T_2G_2$, in which the guanine (G) base at the central loop was replaced with an adenine (A) or inosine (I) base, was examined to determine the role of the central G base in stabilizing the quadruplex. Replacement of the central G base by the I base resulted in a slight decrease in thermal stability. On the other hand, the stability of the G-quadruplex decreased to a significant extent when it was replaced with the A base. The optimized structure of the G-quadruplex, which was obtained by a molecular dynamic simulation, showed that the carbonyl group of the C5 position of the central G base could form hydrogen bonds with the G1 amine group at the C7 position on the upper G-quartet. This formation of a hydrogen bond contributes to the stability of the G-quadruplex. The spectral property of *meso*-tetrakis(*N*-methylpyridium-4yl)porphyrin (TMPyP) associated with the G-quadruplex was characterized by a moderate red shift and hypochromism in the absorption spectrum, a positive CD signal, and two emission maxima in the fluorescence emission spectrum, suggesting that TMPyP binds at the exterior of the G-quadruplex. Spectral properties were slightly altered when the G base at the central loop was replaced with A or I, while the fluorescence decay times of TMPyP associated with the G-quadruplex were identical. Observed spectral properties removes the

* Corresponding author.
E-mail address: seogkim@yu.ac.kr (S.K. Kim).

http://dx.doi.org/10.1016/j.bpc.2015.05.011

possibility of intercalation binding mode for TMPyP. TMPyP binds at the exterior of the quadruplex. Whether it stacks on the central loop or binds at the side of the quadruplex is unclear at this stage.

1. Introduction

Telomeres located at the end of chromosomes protect the chromosomes from deterioration and influences a range of biological processes, such as the prevention of telomerase binding, promoter activation and gene rearrangement [1]. Such biological importance has attracted considerable attention for the structure and dynamics of the G-quadruplex [2–6]. The G-quadruplex contains stretches of guanine bases (G) that are capable of forming a unique structure called the G-quadruplex, which is composed of four G-bases connected via Hoogsteen type hydrogen bonding in the same plane. The stacking interaction between the G bases as well as other electrostatic interaction also helps stabilize the G-quartet in the G-quadruplex in addition to hydrogen bonding. The presence of a monovalent cation, such as K^+ or Na^+ is essential for stabilizing the G-quadruplex [7]. These monovalent cationic ions interact with the carbonyl group of the G bases. A variety of structures depending on the number of G-quartet, nature of loops and central cation have been reported [8–15]. For example, an early NMR study of a thrombin-binding aptamer, $5'G_2T_2G_2TGTG_2T_2G_2$, showed that this DNA adopts a highly compact, high symmetrical structure that consist of tetrads of G base pairs and three loops (Fig. 1) [9]. The loops linking the G quartets on the top or bottom of the G-quadruplex can have various sequences and lengths. The nature of the loops is related to the direction of the G-quartet runs [10,15–18]. For example, a recent single molecule fluorescence technique showed that both the loop length and sequence contribute to the conformation of the G-quadruplex. The folding dynamics also depends on the loop composition [15]. On the other hand, the interaction and the role of the nucleo-bases at the central loop in the stabilization of the G-quadruplex are unclear.

Understanding the binding mode and interaction of metal complexes including metallo-porphyrin derivatives to G quadruplexes is important for identifying rational biological applications of these molecules, such as the development of anticancer drugs [19]. Various binding modes of the free base and metallo-porphyrin have been reported, including the intercalation of planar porphyrin between two adjacent G-quartets [20–26], weak external binding via electrostatic interactions [27–31], and stacking on the external G-tetrads [32–39]. A recent absorption spectrum, circular dichroism (CD) and fluorescence study reported that a representative of the cationic porphyrin family, *meso*-tetrakis(*N*-methylpyridium-4yl)porphyrin (TMPyP, Fig. 1), exhibited an external binding mode to the $5'G_2T_2G_2TGTG_2T_2G_2$ quadruplex [27].

In this study, the role of the G_8 base at the central loop in the stability of the G-quadruplex was investigated by comparing the thermal stability of various G-quadruplexes at which G_8 base was replaced with adenine (A) or inosine base (I) (Fig. 1). The binding mode of TMPyP to G-quadruplexes having different bases at the central loop was also examined by CD and fluorescence decay profiles.

2. Experimental

2.1. Materials and methods

The thrombin-binding aptamer, $5'G_2T_2G_2TXTG_2T_2G_2$ (X = A, I or G), was purchased from SBS Genetech Co., Ltd (China) and TMPyP from Frontier Scientific Inc. (Logan, Utah). They were dissolved in 5 mM cacodylate buffer, pH 7.0, and used for the measurements without further purification. The concentrations of the oligonucleotide and TMPyP were determined spectrophotometrically using the extinction coefficients of $\varepsilon_{421nm} = 2.26 \times 10^5\ M^{-1}\ cm^{-1}$ and $\varepsilon_{260\ nm} = 1.43 \times 10^5\ M^{-1}\ cm^{-1}$ for TMPyP and oligonucleotide, respectively. The quadruplex was formed by the addition of 100 mM KCl followed by heating at 80 °C for 10 min and annealing overnight at room temperature. The formation of the quadruplex was confirmed by its characteristic CD spectrum. The CD spectra were recorded on a Jasco J-810 spectropolarimeter (Tokyo, Japan) and the absorption spectra were obtained on a Cary 100 spectrophotometer (Palo Alto, CA). The temperature was increased by 0.2 °C every 2 min using a built-in peltier at the temperature-dependent CD intensity that reflects the unfolding of the quadruplex. Fluorescence emission spectrum was recorded on an FS-2 fluorimeter at 20 °C (Sinco, Co. Seoul, Korea) with excitation at 421 nm. The silt widths for both excitation and emission were 10/10 nm. The fluorescence decay profiles were measured on an iHR320 TSCPC system constructed at the Center for Research Facilities, Kongju National University. The sample was excited at 405 nm and the emission was detected at 650 nm.

2.2. Computation

All molecular dynamic (MD) simulations were carried out using the CHARMM program with the provisions for calculating multipolar

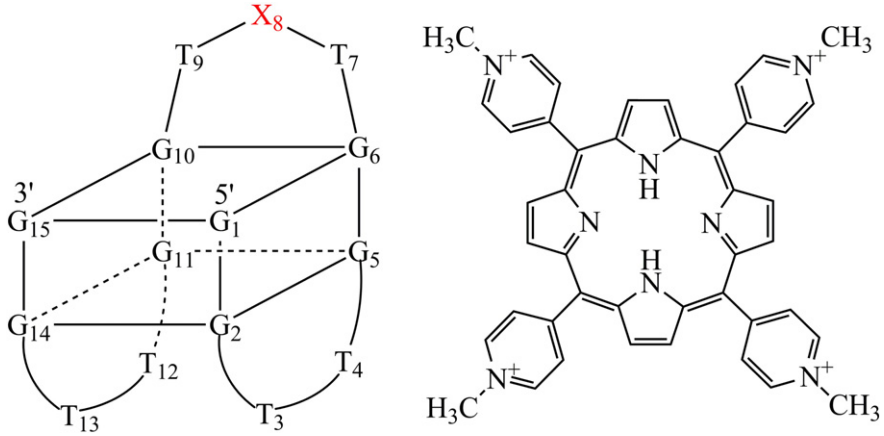

Fig. 1. Schematic diagram of the $5'G_2T_2G_2TXTG_2T_2G_2$ quadruplex (where X = G, A, or I) and the chemical structure of TMPyP.

interactions. The initial structure of the G-quadruplex, 1C34, was obtained from the Protein Data Bank (PDB). The simulations were carried out under spherical boundary conditions (SBC). The initial structure of the G-quadruplex was obtained first by minimizing the total energy using the steepest descent methods for 500 steps; the G-quadruplex was solvated in a cubic water box with a length of 45 Å, containing close to 1000 water molecules. After solvation, the system was optimized, followed by heating to 300 K for 20 ps and equilibration for 20 ps at 300 K. The production simulations in the *NPT* ensemble were conducted using the TIP3P model, which is for water molecules. The TIP3P water was used with SHAKE. Nonbonded interactions (electrostatic interactions and van der Waals interactions) are included. The interaction of distance is less than 10 Å and switched between 10 and 12 Å. After the *NPT* ensemble, the product simulations were carried out by the *NVE* ensemble.

3. Results and discussion

3.1. Thermal unfolding of G-quadruplex

The aptamer 5′$G_2T_2G_2TGTG_2T_2G_2$ exhibited a characteristic CD spectrum in the DNA absorption region with its positive maxima at 294 nm and 248 nm, and negative minimum at 266 nm in the presence of 100 mM KCl at 20 °C (Fig. 2A, insertion), suggesting the formation of an antiparallel type G-quadruplex [27]. At high temperatures (80 °C), the CD spectrum disappeared: a transition from the G-quadruplex to a single stranded oligonucleotide occurred. The shape of the CD spectra at 20 °C were unaffected by the replacement of the central G base by the A or I base (supplementary information, S1). Similarly the CD spectrum at 80 °C was unaffected by replacing the central G base by A or I. The origin of the CD spectrum of the achiral nucleobase from various DNA secondary structures is the chiral arrangement of electric transition moment of the stacked bases in the structure. This suggests that the nature of the purine base at the central loop (position 8) has little effect on the secondary structure of the G-quadruplex.

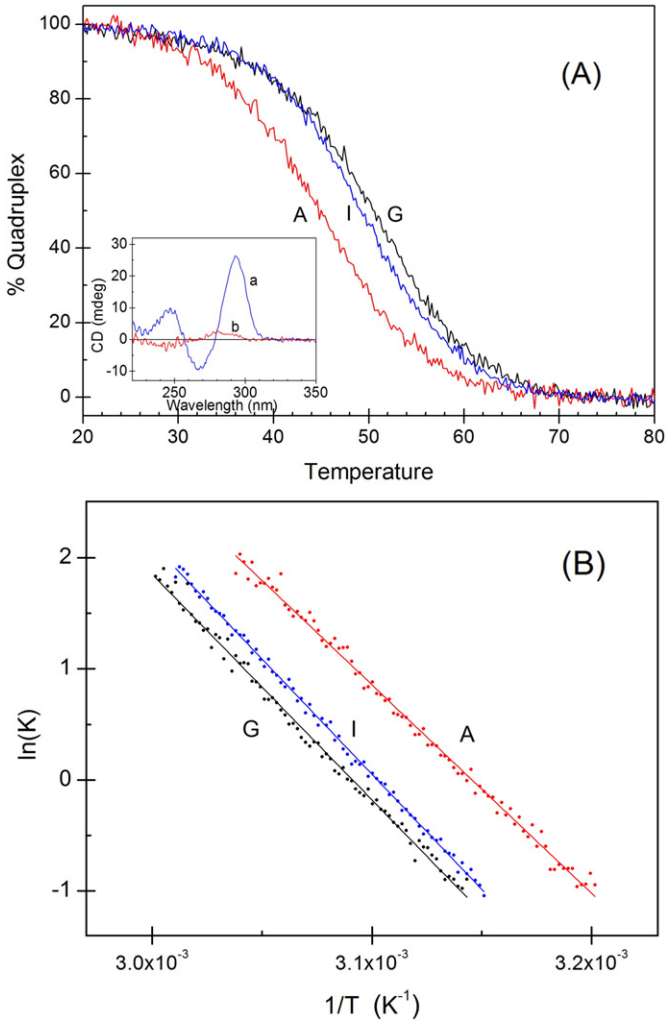

Fig. 2. Temperature-dependent change in CD at 294 nm (A) and the van't Hoff plot (B) for denaturation of the G-quadruplex, 5′$G_2T_2G_2TXTG_2T_2G_2$ (X = A, I or G). The concentration of the G-quadruplex was 5 μM. The CD spectrum of the G-quadruplex (X = G) at 20 °C (curve a) and at 80 °C is inserted in panel (A).

Table 1
Thermodynamic parameters for the thermal dissociation of the G-quadruplex.

Nucleotide	ΔS, J · mol^{-1}	ΔH, kJ · mol^{-1}	$\Delta G_{25\ °C}$, J · mol^{-1}
G	7.55 ± 0.07	2.44 ± 0.02	189
I	7.73 ± 0.04	2.44 ± 0.01	135
A	7.10 ± 0.06	2.26 ± 0.02	143

Fig. 2A shows the change in CD intensity at 294 nm with respect to temperature. Replacing the G base with the A or I base destabilized the G-quadruplex. The temperature at which a 50% transition (T_m) occurred was ~50.8 °C for 5′$G_2T_2G_2TGTG_2T_2G_2$, which is slightly lower than in the previous report [27]. Replacement of the G base at the central loop by the I base, resulted in a slight decrease in T_m, which was observed at ~49.5 °C. A large decrease in T_m was observed when the G base was replaced with the A base: T_m = ~45.0 °C. Considering that the temperature-dependent change in CD reflects the shift in equilibrium from the G-quadruplex to the single stranded 5′$G_2T_2G_2TXTG_2T_2G_2$ aptamer, the equilibrium constant, *K*, can be calculated easily as follows:

$$G\text{-}quadruplex \rightleftharpoons single\ strand, \quad K = \frac{[single\ strand]}{[G\text{-}quadruplex]}.$$

The logarithm of the temperature-dependent equilibrium constant was plotted as a function of the reciprocal absolute temperature to

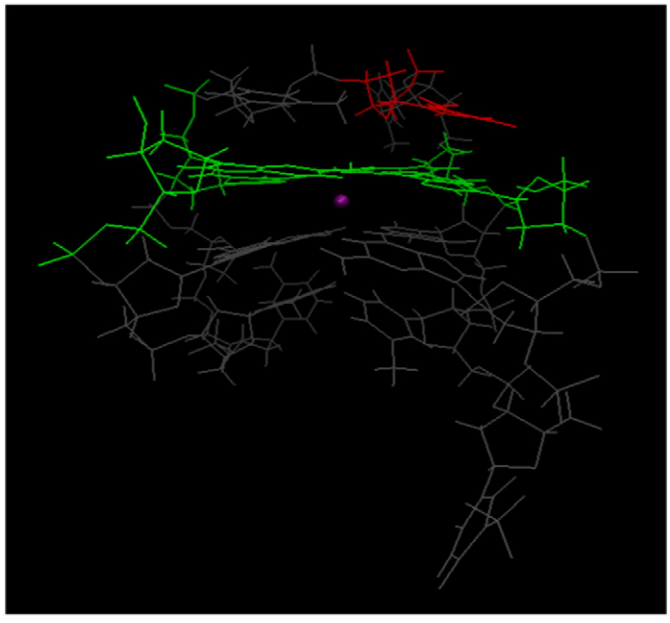

Fig. 3. Energy-minimized structure of the 5′$G_2T_2G_2TGTG_2T_2G_2$ G-quadruplex obtained by a Charmm CHAR (c36a1) program in the presence of an excess of K^+. The upper G-quartet including sugar and phosphate moieties are visualized by a green color, whereas the G base at the central loop is shown in red. The purple dot at the center represents K^+.

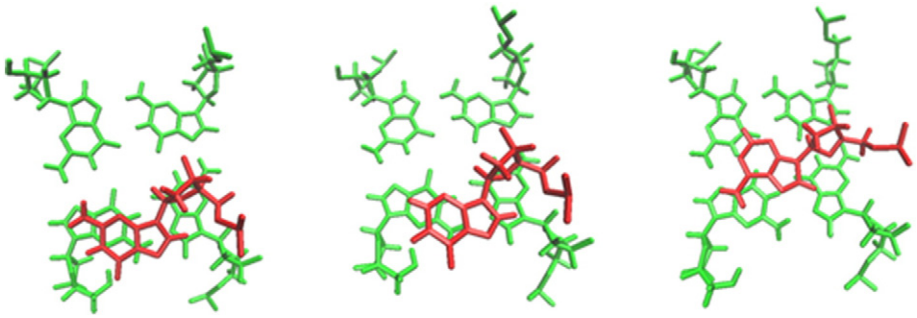

Fig. 4. Top view of the G-quadruplexes to show the stacking between the base of the central loop and upper-G-quartet. From left, X = G, I and A.

give a van't Hoff plot (Fig. 2B), where R is the gas constant and T is the absolute temperature.

$$\ln K = -\frac{\Delta H^{\circ}}{R}\left(\frac{1}{T}\right) + \frac{\Delta S^{\circ}}{R}$$

The enthalpy(ΔH°) and entropy (ΔS°) for unfolding of the G-quadruplex can be calculated from the slope and y-intercept of the plot. Table 1 lists the resulting thermodynamic parameters. As shown in Fig. 2B, unfolding of the G-quadruplexes is endothermic with a negative slope in the van't Hoff plot and the entropy change was positive for all three oligonucleotides. Therefore, the transition from the quadruplex to a single strand is enthalpy driven. The positive Gibb's free energies at 25 °C for all oligonucleotides indicate that the dissociation of the G-quadruplex to a single-strand is non-spontaneous. The Gibb's free energy is the largest for X = G. The slope of the van't Hoff plot shows that the enthalpy changes are positive for all G-quadruplexes. A comparison of X = G and X = I showed that the enthalpy change was identical, whereas the entropy change was larger for X = I than for X = G case. Therefore, the difference in stability between these two quadruplexes originates mainly from the difference in the entropy changes. In the case of X = A, the stability appeared to be similar to X = I with a slightly higher Gibb's free energy. The significantly low enthalpy change appears to be the main reason for the lower stability of the X = A quadruplex compared to that of the X = G quadruplex.

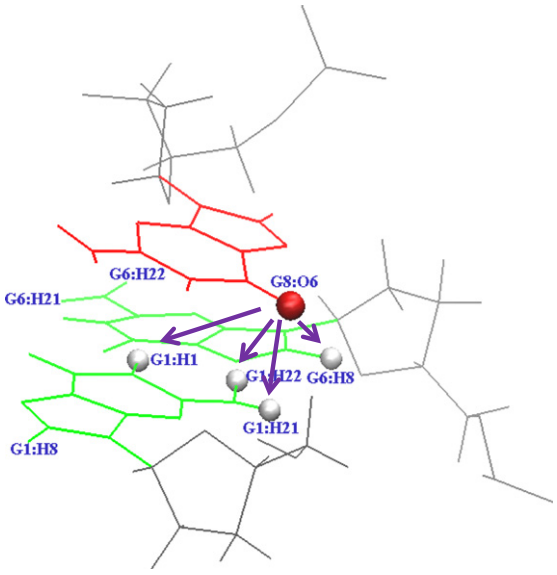

Fig. 5. Enlarged view showing the carbonyl group of the G base (G8: O6, red ball) at the central loop and a possible hydrogen bond forming atoms (gray balls). The hydrogen atoms that possibly form a hydrogen bond with the carbonyl group of the central G base are denoted by arrows.

3.2. Structure of the G-quadruplex with X = G, A or I

The crystal and in-solution structures of the G-quadruplex formed from the thrombin-binding DNA aptamer, $5'G_2T_2G_2TGTG_2T_2G_2$, have been reported by nuclear magnetic resonance (NMR) spectroscopy and X-ray crystallography [8–10]. The aptamer adopts a highly compact symmetrical structure which consists of two G-quartet and three loops. The energy-minimization study performed using the Charmm CHAR (c36a1) program in the presence of an excess of K^+ ion showed that the $5'G_2T_2G_2TGTG_2T_2G_2$ oligonucleotides had a similar structure (Fig. 3). The loop length and sequence contribute to the conformation of the G-quadruplex [15]. Replacement of the central G by A or I also alter the overall structure (Supporting information S2), particularly the lower G-quartet. The carbonyl part of all four G bases near the center tilt to a large extent at the lower G-quartet, whereas the extent of the tilt is less for those cases of X = A or = I. Nevertheless, a detailed analysis of the overall structure was beyond the scope of this study. The G bases that form the upper G-quartet are in the same plane. The molecular plane of the central bases i.e., G, A or I was almost parallel to the plane of the upper G-quartet, suggesting the possibility of a stacking interaction between the upper G-quartet and central base. Fig. 4 depicts the top view of the upper G-quartet and the central purine bases. The phosphate moieties are not shown for clarity. In the X = G and = I cases, a large overlap of the base plane of the central G and I base with G1 and G6 at the upper G-quartet, was found. The carbonyl group at the C5 position of the G and I base is found toward the side of the G-quadruplex. On the other hand, the A base moved toward the center of the upper G-quartet when X = A. In view of Fig. 4, it is clear that the central G base has slightly more stacking overlap than I, while A has poor stacking, Therefore, the difference in the extent of overlap, i.e., stacking interaction between the central base and the G bases at the upper G-quartet contributes, at least in part, to the thermal stability of the G-quadruplex.

In the I base case, the amine group of G base at the C7 position was missing, whereas the carbonyl group at C5 was replaced with an amine group in the A base case. Considering that the position of the I base relative to G1 and G6 is similar to that of the G base, the contribution of the C7 amine group in determining the conformation of the central loop is minimal. When the carbonyl group of the G base, which is a hydrogen acceptor in the hydrogen bond was replaced with an amine

Table 2
Distance (Å) of H atoms at the vicinity of the oxygen atom at the G8 carbonyl group.

Residue	G	I
G1H21	3.1509	4.1947
G1H22	4.1127	4.1564
G1H1	5.0604	5.4650
G1H8	6.8983	9.6040
G6H21	10.9032	8.6322
G6H22	11.0308	5.5296
G6H1	8.9810	7.0281
G6H8	5.5707	3.9252

group, a hydrogen donor, significant relocation of the central base occurs. This highlights the importance of the carbonyl group of the G base at the central loop. Fig. 5 shows the G base at the central loop and H atoms at the vicinity from which the formation of a hydrogen bond is possible. Table 2 lists the distances between the oxygen atom of the carbonyl group and the neighboring hydrogen atoms. The distance between hydrogen atoms at the C7 amine group of the G1 base and the oxygen atom of the carbonyl group of the G8 base were 3.1509 and 4.1127 Å, which appear to be near enough to form a hydrogen bond in the X = G case. In the X = I case, however, the distances were 4.1947 and 4.1564 Å. The T_m for $5'G_2T_2G_2TGTG_2T_2G_2$ was ~50.8 °C, whereas that of $5'G_2T_2G_2TITG_2T_2G_2$ was ~49.5 °C. The carbonyl group, which possibly forms a hydrogen bond, is missing in the X = A case, which causes, at least in part, the instability of the G-quadruplex. The observed T_m for the X = A case was ~45.0 °C. On the other hand, the C7 amine group had negligible effects on stabilizing the G-quadruplex because an absence of this group did not alter the T_m significantly as shown for the X = G and X = I cases. Therefore, this difference in the distance can be the reason for the G-quadruplex with X = I being slightly less stable than the X = G case, in addition to the difference in the stacking interaction.

3.3. Binding mode of TMPyP

Cationic porphyrins have been used as a probe for the structure and dynamics of various G-quadruplexes. In this study, TMPyP (Fig. 1) was used as a probe to examine the effects of various purine bases at the central loop. All spectral properties including the absorption, CD and fluorescence emission spectra reported in this section were measured at [TMPyP]/[G-quadruplex] ratios of 0.1, 0.2, 0.4, 0.6, 0.8, and 1.0. The mixing ratio for the fluorescence decay profile was 0.5. The measured spectral properties were invariant regardless of the mixing ratios, suggesting that the binding mode of TMPyP to the G-quadruplex is homogeneous at these ratios. Therefore, only those obtained at the [TMPyP]/[G-quadruplex] = 1.0 are presented in this section for clarity. Fig. 6(A) presents the absorption spectrum of TMPyP in the Soret absorption region in the presence and absence of the G-quadruplex. When associated with the X = G quadruplex, TMPyP produced a 5 nm red shift (from 422 nm to 427 nm) and ~20% hypochromism, which is in agreement with a previous study, but in contrast to that of the fully intercalated TMPyP between the base pairs of double stranded DNA. In the latter case, a ~20 nm red shift and ~47% hypochromism were reported [27]. Small variations in the absorption spectrum were observed when the G base was replaced with the A or I base. In the X = I quadruplex case, a small additional hypochromism and a 6 nm red shift was produced, whereas the X = A quadruplex showed no further shift and the largest hypochromism. On the other hand, the observed variations in the absorption spectra according to the nature of the base at position X were too small to reflect the large change in the binding mode of TMPyP. Rather, it should be accepted as a sign of a delicate change in the environment of the TMPyP binding site. The CD spectrum is a sensitive tool for examining the binding mode of TMPyP to various DNAs. Achiral porphyrins induces a CD signal upon binding to double stranded DNAs because of the interaction of the B_x and B_y electric transition

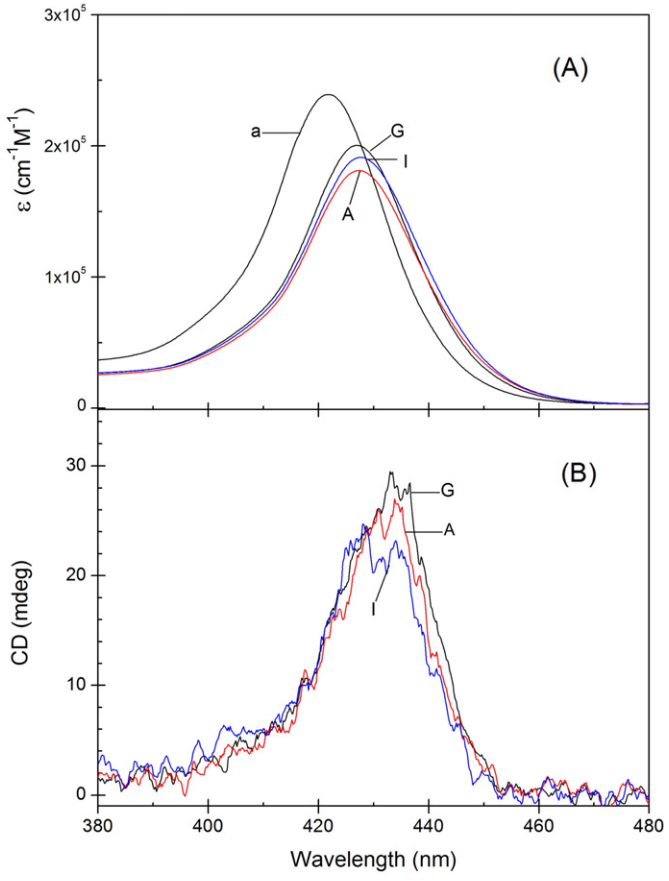

Fig. 6. (A) Absorption and (B) CD spectra of the TMPyP complexed with G-quadruplex. The absorption spectrum of quadruplex-free TMPyP is marked by curve a (Panel (A)). The G-quadruplex with a different base at the central loop is denoted as G, A, and I. [TMPyP]/[quadruplex] = 1. [Quadruplex] = 5 μM.

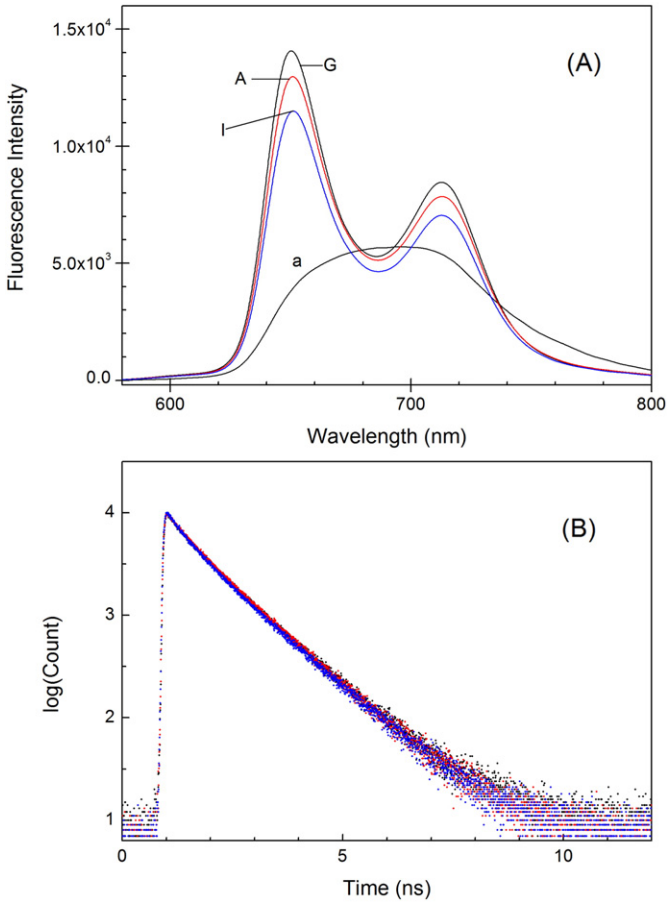

Fig. 7. Fluorescence emission spectra of TMPyP in the absence (curve a) and presence of the G-quadruplex. The base at the central loop is denoted by G, A and I, respectively. (B) Fluorescence decay time of TMPyP complexed with G-quadruplexes. The decay profiles were identical for all three G-quadruplexes. [TMPyP]/[G-quadruplex] = 1. [G-quadruplex] = 0.5 μM. The excitation wavelength was 421 nm for recording of the emission spectrum. The slit widths were 10 nm for both excitation and emission windows. The fluorescence decay profiles were recorded at 405 nm excitation and at 650 nm emission.

moments of porphyrin and those of chirally-arranged DNA bases. In the double stranded DNA case, a negative CD band in the Soret band was considered to be diagnostic of the intercalation of porphyrin between the DNA base pairs, whereas a positive band may reflect the external binding mode [40,41]. Fig. 6(B) shows the CD spectrum of the TMPyP bound to the G-quadruplexes at [TMPyP]/[G-quadruplex] = 1.0. For all G-quadruplexes, i.e., X = G, A, or I, a positive CD spectrum in the Soret region centered at ~430 nm was apparent. Cationic porphyrins with axial ligands produced similar positive CD spectra [27] when bound to the same G-quadruplex, indicating that TMPyP is not intercalated between the G-quartet. The identical CD spectrum shows that changing the G base to A or I did not affect the binding mode of TMPyP.

Fig. 7(A) and 7(B) show the fluorescence emission spectrum and decay profiles of TMPyP associated with the X = G, A and I quadruplex, respectively. Although a broad emission band between 620–800 nm was produced for TMPyP in the absence of the G-quadruplex when excited at the Soret region, two maxima at 650 nm and 713 nm were apparent when associated with the X = G, A or I G-quadruplex. Although small variations in the fluorescence intensity was observed, the appearance of the emission spectrum was essentially the same for X = G, A and I G-quadruplex, suggesting that, in addition to the absorption and CD spectrum, the change in the central G base at the loop did not alter the binding mode of TMPyP. The conversion of the featureless emission spectrum of DNA-free TMPyP to two emission bands of DNA-bound TMPyP is normally assigned to the conversion of self-associated porphyrin in an aqueous solution to monomeric DNA bound species. TMPyP in aqueous solution was reported to exhibit two fluorescence decay times, 2.18 ns and 5.37 ns. The short component is normally assigned to TMPyP adsorbed at the surface of the quartz cuvette. Upon binding to the G-quadruplex, the long decay time increased to 8.76 ns [27,33]. The decay profile presented for the TMPyP complexed with the X = G quadruplex in Fig. 7(B) exhibited similar behavior. The point is that the fluorescence decay profiles of TMPyP remain when the X base at the central loop is replaced with either A or I. The fluorescence decay of TMPyP associated with X = G, A or I produced precisely the same profiles.

As mentioned previously, various types of binding of cationic porphyrins to the G-quadruplex produced a variety of binding modes including the intercalation of planar porphyrin between the two adjacent G-quartets [20–26], weak external binding [27–31], and stacking on the external G-tetrads [32–39] have been reported. The spectral properties of TMPyP associated with the G-quadruplexes can be summarized as a relatively small red shift and hypochromism in the absorption spectrum, a positive CD band and fluorescence emission spectrum with two clear maxima. These properties remove the possibility of intercalative binding. Whether TMPyP stacks on the external TGT central loop or binds at the side of the G-quadruplex is unclear at this stage because the effect of replacing the G base with A or I on the binding property was minimal.

4. Conclusion

The carbonyl group at the C5 position of the G base located at the central loop contribute to the stability of the thrombin-binding 5′ $G_2T_2G_2TGTG_2T_2G_2$ aptamer, conceivably by forming hydrogen bonds with the nearby H atoms at the C7 amine group of the G1 base. Replacement of this G base with A or I base did not alter the binding mode of TMPyP significantly.

Acknowledgment

This study was supported by the Korea Research Foundation (Grant no. NRF 2012–008875).

Appendix A. Supplementary data

Supplementary data to this article can be found online at http://dx.doi.org/10.1016/j.bpc.2015.05.011.

References

[1] Y. Wu, R.B. Broch Jr., G-quadruplex nucleic acids and human disease, FEBS J. 277 (2010) 3470–3488.
[2] J.L. Huppert, Structure, location and interactions of G-quadruplexes, FEBS J. 277 (2010) 3452–3458.
[3] H.J. Lipps, D. Rhodes, G-quadruplex structures: *in vivo* evidence and function, Trends Cell Biol. 19 (2009) 414–422.
[4] S. Burge, G.N. Parkinson, P. Hazel, A.K. Todd, S. Neidle, Quadruplex DNA: sequence, topology and structure, Nucleic Acids Res. 34 (2006) 5402–5415.
[5] J.L. Huppert, Hunting G-quadruplexes, Biochimie 90 (2008) 1140–1148.
[6] N. Maizels, Dynamic roles for G4 DNA in the biology of eukaryotic cells, Nat. Struct. Mol. Biol. 13 (2006) 1055–1059.
[7] L. Ying, J.J. Green, H. Li, D. Klenerman, S. Balasubramanian, Studies on the structure and dynamics of the human telomeric G quadruplex by single-molecule fluorescence resonance energy transfer, Proc. Natl. Acad. Sci. U. S. A. 100 (2003) 14629–14634.
[8] R.F. Macaya, P. Schultze, F.W. Smith, J.A. Roe, J. Feigon, Thrombin-binding DNA aptamer forms a unimolecular quadruplex structure in solution, Proc. Natl. Acad. Sci. U. S. A. 90 (1993) 3745–3749.
[9] K.Y. Wang, S. McCurdy, R.G. Shea, S. Swaminathan, P.H. Bolton, A DNA aptamer which binds to and inhibits thrombin exhibits a new structural motif for DNA, Biochemistry 32 (1993) 1899–1904.
[10] K. Padmanabhan, K.P. Padmanabhan, J.D. Ferrara, J.E. Sadler, A. Tulinsky, A. The structure of alpha-thrombin inhibited by a 15-mer single-stranded DNA aptamer, J. Biol. Chem. 268 (1993) 17651–17654.
[11] G.N. Parkinson, M.P.H. Lee, S. Neidle, Crystal structure of parallel quadruplexes from human telomeric DNA, Nature 417 (2002) 876–880.
[12] S. Burge, G.N. Parkinson, P. Hazel, A.K. Todd, S. Neidle, Quadruplex DNA: sequence, topology and structure, Nucleic Acids Res. 34 (2006) 5402–5415.
[13] D.J. Patel, A.T. Phan, V. Kuryavyi, Human telomere, oncogenic promoter and 5′-UTR G-quadruplexes: diverse higher order DNA and RNA targets for cancer therapeutics, Nucleic Acids Res. 35 (2007) 7429–7455.
[14] K.W. Lim, S. Amrane, S. Bouaziz, W. Xu, Y. Mu, D.J. Patel, K.N. Luu, A.T. Phan, Structure of the human telomere in K^+ solution: a stable basket-type G-quadruplex with only two G-tetrad layers, J. Am. Chem. Soc. 131 (2009) 4301–4309.
[15] R. Tippana, W. Xiao, S. Myong, G-quadruplex conformation and dynamics are determined by loop length and sequence, Nucleic Acids Res. 42 (2014) 8106–8114.
[16] Y. Wang, D.J. Patel, Solution structure of the human telomeric repeat $d[AG_3(T_2AG_3)_3]$ G-tetraplex, Structure 1 (1993) 263–282.
[17] A.T. Phan, K.L. Luu, D.J. Patel, Different loop arrangements of intramolecular human telomeric (3 + 1) G-quadruplexes in K^+ solution, Nucleic Acids Res. 34 (2006) 5715–5719.
[18] P. Hazel, J.L. Huppert, S. Balasubramanian, S. Neidle, Loop-length-dependent folding of G-quadruplexes, J. Am. Chem. Soc. 126 (2004) 16405–16415.
[19] S.N. Georgiades, N.H. Abd Karim, K. Suntharalingam, Interaction of metal complexes with G-quadruplex DNA, Angew. Chem. Int. Ed. 49 (2010) 4020–4034.
[20] M. Cavallari, A. Garbesi, R.D. Felice, Porphyrin intercalation in G4-DNA quadruplexes by molecular dynamics simulations, J. Phys. Chem. B 113 (2009) 13152–13160.
[21] C. Wei, G. Jia, J. Zhou, G. Han, C. Li, Evidence for the binding mode of porphyrins to G-quadruplex DNA, Phys. Chem. Chem. Phys. 11 (2009) 4025–4032.
[22] M. Del Toro, R. Gargallo, R. Eritja, J. Jaumot, Study of the interaction between the G-quadruplex-forming thrombin-binding aptamer and the porphyrin 5,10,15,20-tetrakis-(N-methyl-4-pyridyl)-21,23H-porphyrin tetratosylate, Anal. Biochem. 379 (2008) 8–15.
[23] I. Lubitz, N. Borovok, A. Kotlyar, Interaction of monomolecular G4-DNA nanowires with TMPyP: evidence for intercalation, Biochemistry 46 (2007) 12925–12929.
[24] C. Wei, G. Jia, J. Yuan, Z. Feng, C. Li, A spectroscopic study on the interactions of porphyrin with G-quadruplex DNAs, Biochemistry 45 (2006) 6681–6691.
[25] I. Haq, J.O. Trent, B.Z. Chowdhry, T.C. Jenkins, Intercalative G-tetraplex stabilization of telomeric DNA by a cationic porphyrin, J. Am. Chem. Soc. 121 (1999) 1768–1779.
[26] N.V. Anantha, M. Azam, R.D. Sheardy, Porphyrin binding to quadruplexed T_4G_4, Biochemistry 37 (1998) 2709–2714.
[27] Y.-H. Kim, C. Lee, S.K. Kim, S.C. Jeoung, Interaction of metallo- and free base meso-tetrakis(N-methylpyridium-4-yl)porphyrin with a G-quadruplex: effect of the central metal ions, Biophys. Chem. 190–191 (2014) 17–24.
[28] A. Arora, S. Maiti, Effect of loop orientation on quadruplex–TMPyP4 interaction, J. Phys. Chem. B 112 (2008) 8151–8159.
[29] K. Halder, S. Chowdhury, Quadruplex-coupled kinetics distinguishes ligand binding between G4 DNA motifs, Biochemistry 46 (2007) 14762–14770.
[30] J. Seenisamy, S. Bashyam, V. Gokhale, H. Vankayalapati, D. Sun, A. Siddiqui-Jain, N. Streiner, K. Shin-Ya, E. White, E.W.D. Wilson, L.H. Hueley, Design and synthesis of an expanded porphyrin that has selectivity for the c-MYC G-quadruplex structure, J. Am. Chem. Soc. 127 (2005) 2944–2959.
[31] T. Yamashita, T. Uno, Y. Ishikawa, Stabilization of guanine quadruplex DNA by the binding of porphyrins with cationic side arms, Bioorg. Med. Chem. 13 (2005) 2423–2430.

[32] A.J. Bhattacharjee, K. Ahluwalia, S. Taylor, O. Jin, J.M. Nicoludis, R. Buscaglia, J.B. Chaires, D.J.P. Kornfilt, D.G.S. Marquardt, L.A. Yatsunyk, Biochimie 93 (2011) 1297–1309.
[33] C. Wei, L. Wang, J. Jia, G. Zhou, C. Han, C. Li, The binding mode of porphyrins with cation side arms to (TG4T)4 G-quadruplex: spectroscopic evidence, Biophys. Chem. 143 (2009) 79–84.
[34] J. Pan, S. Zhang, Interaction between cationic zinc porphyrin and lead ion induced telomeric guanine quadruplexes: evidence for end-stacking, J. Biol. Inorg. Chem. 14 (2009) 401–407.
[35] G. Jia, Z. Feng, C. Wei, J. Zhou, X. Wang, C. Li, Dynamic insight into the interaction between porphyrin and G-quadruplex DNAs: time-resolved fluorescence anisotropy study, J. Phys. Chem. B 113 (2009) 16237–16245.
[36] G.N. Parkinson, R. Ghosh, S. Neidle, Structural basis for binding of porphyrin to human telomeres, Biochemistry 46 (2007) 2390–2397.
[37] S.E. Evans, M.A. Mendez, K.B. Turner, L.R. Keating, R.T. Grimes, S. Melchoir, V.A. Szalai, End-stacking of copper cationic porphyrins on parallel-stranded guanine quadruplexes, J. Biol. Inorg. Chem. 12 (2007) 1235–1249.
[38] L.R. Keating, V.A. Szalai, Parallel-stranded guanine quadruplex interactions with a copper cationic porphyrin, Biochemistry 43 (2004) 15891–15900.
[39] H. Han, D.R. Langley, A. Rangan, L.H. Hurley, Selective interactions of cationic porphyrins with G-quadruplex structures, J. Am. Chem. Soc. 123 (2001) 8902–8913.
[40] L. Gong, I. Bae, S.K. Kim, Effect of axial ligand on the binding mode of M-meso-tetrakis(N-methylpyridinium-4-yl)porphyrin to DNA probed by circular and linear dichroism spectroscopies, J. Phys. Chem. B 116 (2012) 12510–12521.
[41] Y.R. Kim, L. Gong, J.J. Park, Y.J. Jang, J. Kim, S.K. Kim, Systematic investigation on the central metal ion dependent binding geometry of M-meso-tetrakis(N-methylpyridinium-4-yl)porphyrin to DNA and their efficiency as an acceptor in DNA-mediated energy transfer, J. Phys. Chem. B 116 (2012) 2330–2337.